# Volatile Glycosylation in Tea Plants: Sequential Glycosylations for the Biosynthesis of Aroma β-Primeverosides Are Catalyzed by Two *Camellia sinensis* Glycosyltransferases[1][OPEN]

**Shoji Ohgami[2], Eiichiro Ono[2]*, Manabu Horikawa, Jun Murata, Koujirou Totsuka, Hiromi Toyonaga, Yukie Ohba[3], Hideo Dohra, Tatsuo Asai, Kenji Matsui, Masaharu Mizutani, Naoharu Watanabe, and Toshiyuki Ohnishi***

Graduate School of Agriculture (S.O., K.T., Y.O., T.A., T.O.) and Research Institute of Green Science and Technology (H.D., T.O.), Shizuoka University, Shizuoka 422–8529, Japan; Research Institute, Suntory Global Innovation Center, Shimamoto, Mishima, Osaka 618–8503, Japan (E.O., H.T.); Bioorganic Research Institute, Suntory Foundation for Life Sciences, Shimamoto, Mishima, Osaka 618–8503, Japan (M.H., J.M.); Graduate School of Medicine, Yamaguchi University, Yamaguchi 753–8515, Japan (K.M.); Graduate School of Agricultural Science, Kobe University, Kobe 657–8501, Japan (M.M.); and Graduate School of Engineering, Shizuoka University, Hamamatsu 432–8561, Japan (N.W.)

**ORCID IDs: 0000-0002-4875-5176 (K.M.); 0000-0001-6862-9639 (T.O.).**

Tea plants (*Camellia sinensis*) store volatile organic compounds (VOCs; monoterpene, aromatic, and aliphatic alcohols) in the leaves in the form of water-soluble diglycosides, primarily as β-primeverosides (6-*O*-β-D-xylopyranosyl-β-D-glucopyranosides). These VOCs play a critical role in plant defenses and tea aroma quality, yet little is known about their biosynthesis and physiological roles in planta. Here, we identified two UDP-glycosyltransferases (UGTs) from *C. sinensis*, UGT85K11 (CsGT1) and UGT94P1 (CsGT2), converting VOCs into β-primeverosides by sequential glucosylation and xylosylation, respectively. CsGT1 exhibits a broad substrate specificity toward monoterpene, aromatic, and aliphatic alcohols to produce the respective glucosides. On the other hand, CsGT2 specifically catalyzes the xylosylation of the 6′-hydroxy group of the sugar moiety of geranyl β-D-glucopyranoside, producing geranyl β-primeveroside. Homology modeling, followed by site-directed mutagenesis of CsGT2, identified a unique isoleucine-141 residue playing a crucial role in sugar donor specificity toward UDP-xylose. The transcripts of both *CsGTs* were mainly expressed in young leaves, along with *β-PRIMEVEROSIDASE* encoding a diglycoside-specific glycosidase. In conclusion, our findings reveal the mechanism of aroma β-primeveroside biosynthesis in *C. sinensis*. This information can be used to preserve tea aroma better during the manufacturing process and to investigate the mechanism of plant chemical defenses.

Plants emit volatile organic compounds (VOCs), such as monoterpenes (C10), sesquiterpenes (C15), phenylpropanoids (C9), norisoprenoids (C16), aromatic esters, or green leaf alcohols (C6), in response to attacks by insect herbivores, mechanical wounding, or endogenous developmental cues. In general, VOCs are considered not only to be chemical defense compounds transmitting biological signals to the environment (Arimura et al., 2009) but also important commercial products, because they influence the quality and character of dietary foods and beverages as aromas. Tea, manufactured from *Camellia sinensis* (Fig. 1A), is the most popular beverage in the world and is classified as black, green, or oolong tea based on the manufacturing process (withering, rolling, and fermentation), which affects the composition and quantity of aroma compounds (Graham, 1992; Balentine et al., 1997). For instance, black tea is produced by full fermentation, during which tea metabolites artificially react with endogenous enzymes (e.g. polyphenol oxidases and β-glucosidases). Floral tea aroma is one of the crucial components to evaluate the value and quality of tea products. The floral aroma caused by linalool, geraniol, 2-phenylethanol (2-PE), and benzyl alcohol are predominant flavor volatile compounds in oolong tea

[1] This work was supported by the Japan Society for the Promotion of Science (KAKENHI grant no. 26870252 to T.O.) and by Suntory Holdings (to E.O).

[2] These authors contributed equally to the article.

[3] Present address: Bioorganic Research Institute, Suntory Foundation for Life Sciences, Shimamoto, Mishima, Osaka 618–8503, Japan.

* Address correspondence to eiichiro_ono@suntory.co.jp and dtonish@ipc.shizuoka.ac.jp.

The author responsible for distribution of materials integral to the findings presented in this article in accordance with the policy described in the Instructions for Authors (www.plantphysiol.org) is: Toshiyuki Ohnishi (dtonish@ipc.shizuoka.ac.jp).

E.O. and T.O. conceived the project and designed the research; S.O., E.O., M.H., J.M., K.T., H.T., Y.O., H.D., T.A., and T.O. performed the research; S.O., E.O., M.H., J.M., N.W., and T.O. analyzed the data; E.O., J.M., K.M., M.M., and T.O. wrote the article.

[OPEN] Articles can be viewed without a subscription.

www.plantphysiol.org/cgi/doi/10.1104/pp.15.00403

 

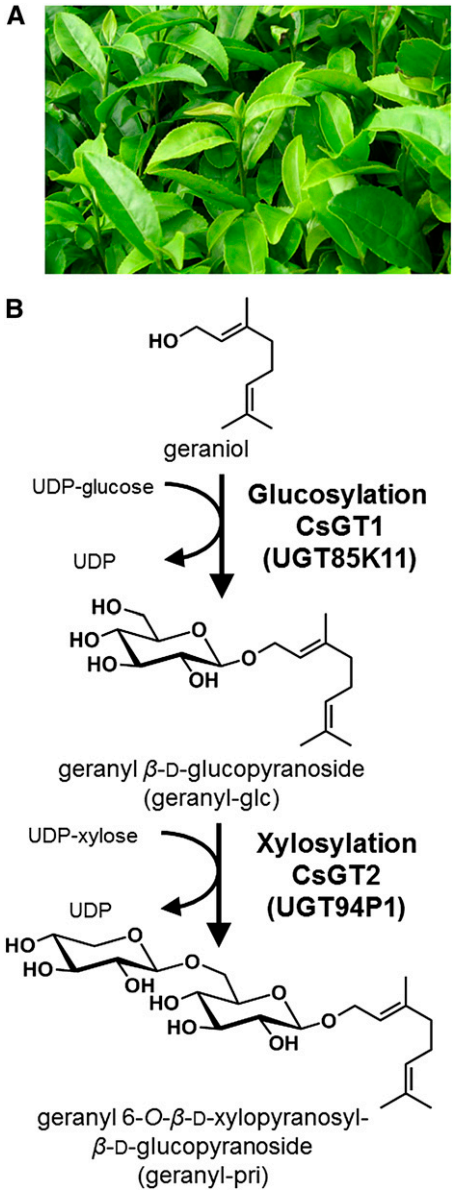


**Figure 1.** Metabolism of VOCs in tea leaves. A, Photograph of young leaves. B, Biosynthesis pathway of geranyl β-primeveroside from geraniol. CsGT1 (UGT85K11) and CsGT2 (UGT94P1) are the two glycosyltransferases that are shown to catalyze the sequential glucosylation and xylosylation of geraniol, respectively, in this work (thick arrows).

and black tea, whereas (*Z*)-3-hexenol adds a grassy note to green tea (Kawakami et al., 1995; Kumazawa and Masuda, 2002). However, fresh leaves of *C. sinensis* barely emit a slightly green note before they are processed for tea. This is because aroma volatiles in tea leaves are accumulated typically as the water-soluble glycoside form. Since the first report on the isolation of benzyl β-D-glucopyranoside (Yano et al., 1991), various aroma glycosides have been identified in fresh tea leaves (Kobayashi et al., 1994). The chemical structure of most glycosides was shown to be β-primeveroside (6-*O*-β-D-xylopyranosyl-β-D-glucopyranoside; Guo et al., 1993, 1994; Moon et al., 1994, 1996), suggesting that a common biosynthetic machinery exists for the conjugation of β-primeveroside to aroma volatiles. A previous quantitative analysis of aroma glycosides in tea leaves demonstrated that levels of aroma β-primeverosides are 3-fold higher than monoglycosides (Wang et al., 2000), indicating that sequential sugar-conjugating reactions to aroma volatiles (glucosylation followed by xylosylation) occur in tea leaves. Highly diverse aroma volatiles, such as benzyl alcohol, 2-PE, (*Z*)-3-hexenol, linalool, and geraniol, are stored as β-primeverosides in tea leaves (Guo et al., 1993, 1994; Moon et al., 1994, 1996). Aromatic alcohols, such as benzyl alcohol and 2-PE, serve as attractants for both parasitic and predatory insects for herbivores, and (*Z*)-3-hexenol released from herbivore-damaged tissue has also been found to induce defense responses in neighboring plants (Pichersky and Gershenzon, 2002; Sugimoto et al., 2014). Monoterpene alcohols such as geraniol and linalool have potential activity toward microorganisms and fungi, and geraniol also has a potent apoptosis-inducing activity in plant cells (Pattnaik et al., 1997; Izumi et al., 1999). Mizutani et al. (2002) reported that a β-PRIMEVEROSIDASE (β-PD) from *C. sinensis* specifically hydrolyzes aroma β-primeverosides into primeverose (disaccharide unit) and aroma volatile (aglycone unit). These data support the idea that aroma β-PD is the key enzyme responsible for the production of chemical defense compounds against pathogens and herbivores as well as for the characteristic aromas of tea products. Thus, it is of particular interest to understand the biosynthesis and physiological role of aroma β-primeverosides in *C. sinensis*. However, corresponding genes for the biosynthesis of volatile β-primeverosides have so far not been reported.

Previous attempts to overproduce volatile compounds in plants by overexpressing genes that are responsible for the biosynthesis of aglycones often resulted in the accumulation of respective glycosides. For example, ectopic expression of *Clarkia breweri* (*S*)-LINALOOL SYNTHASE (LIS) in *Petunia hybrida* resulted in the accumulation of (*S*)-linalyl β-D-glucopyranosides [(*S*)-linalyl-glc; Lücker et al., 2001], and transgenic Arabidopsis (*Arabidopsis thaliana*) plants expressing a strawberry (*Fragaria* × *ananassa*) *NEROLIDO SYNTHASE1* (*FaNES1*) produced (*S*)-linalool, nerolidol, and the glycosylated derivatives (Aharoni et al., 2003). Moreover, relieving a bottleneck in the endogenous eugenol pathway by heterologous overexpression of a *P. hybrida* coniferyl alcohol acetyltransferase gene resulted in up to 7- and 22-fold increases in the levels of eugenol and its glycoside (eugenyl-glc), respectively, in leaves of transgenic aspen (*Populus* spp.; Koeduka et al., 2013). These results suggest that glycosylation of volatiles is a general phenomenon in land plants.

Here, we demonstrate the biochemical and molecular characteristics of two UDP-glycosyltransferases (UGTs) from *C. sinensis*, UGT85K11 (CsGT1) and UGT94P1 (CsGT2), responsible for the sequential glucosylation and xylosylation in the biosynthesis of volatile β-primeverosides (Fig. 1B). In addition, we discuss the physiological roles that volatile metabolites might play in plants, based on

the distribution of aroma precursors and the spatiotemporal expression pattern of these UGT genes in *C. sinensis*.

## RESULTS

### Organ-Specific Composition in Aroma Monoglycosides and Diglycosides

Aroma monoglycosides and diglycosides were extracted from fresh leaves and stems at two developmental stages (young and mature) of *C. sinensis*. Various β-primeverosides, as well as monoglycosides of aroma compounds in tea leaves, were quantified by liquid chromatography (LC)-mass spectrometry (MS; Fig. 2). The results show that geranyl β-primeveroside (geranyl-pri) and linalyl β-primeveroside (linalyl-pri) were the two primary aroma glycosides that were detected mainly in young organs, leaves and stems, respectively. These data also suggest that the metabolic activity of the glycosylation machinery responsible for the biosynthesis of aroma β-primeverosides is higher in growing young tissues. As the tea leaves grew, the total amounts of 2-phenylethyl β-primeveroside (2PE-pri), benzyl β-primeveroside (benzyl-pri), and (*Z*)-3-hexenyl β-primeveroside (hexenyl-pri) increased in the mature leaves, whereas

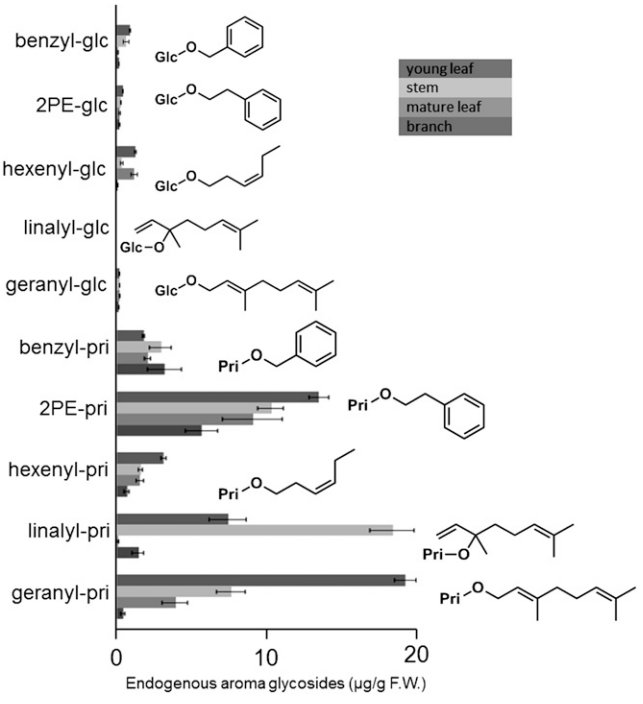


**Figure 2.** Quantification of aroma monoglycosides and diglycosides in fresh tea leaves. Ten glycosides were used as authentic standards to quantify endogenous glycoside in young leaves, young stems, mature leaves, and mature stems of *C. sinensis*: benzyl β-D-glucopyranoside (benzyl-glc), benzyl β-primeveroside (benzyl-pri), geranyl β-D-glucopyranoside (geranyl-glc), geranyl β-primeveroside (geranyl-pri), (*Z*)-3-hexenyl β-D-glucopyranoside (hexenyl-glu), (*Z*)-3-hexenyl β-primeveroside (hexenyl-pri), linalyl-glc, linalyl β-primeveroside (linalyl-pri), 2-phenylethyl β-D-glucopyranoside (2PE-glc), and 2-phenylethyl β-primeveroside (2PE-pri). Data are presented as means ± SD ($n$ = 3). F.W., Fresh weight.

those of geranyl-pri and linalyl-pri decreased (Supplemental Table S1). Since the overall fresh weight of the mature leaves was approximately 4 times larger than that in young leaves, the apparent concentrations of geranyl-pri and linalyl-pri were substantially decreased in mature leaves. These results suggested that these two β-primeverosides were further metabolized to unknown chemical forms or were transferred from young leaves to other parts of the plant.

### Identification of Arabidopsis UGT85A3 Showing Transglucosylation Activity toward Volatiles

The concurrent occurrence of monoglucosides and primeverosides of the corresponding volatiles in tea leaves suggested that primeverosides are biosynthesized via two sequential glycosylations steps, an initial glucosylation followed by xylosylation, rather than by direct conjugation of the primeverosyl moiety to the volatiles. Therefore, we searched for glucosyltransferases potentially responsible for the first glucosylation step in aroma β-primeveroside biosynthesis. For several classes of specialized metabolites, the biosynthetic genes are often coexpressed (Fukushima et al., 2011). Transcriptome expression profiles and coexpression analysis became powerful tools for the prediction of the biosynthetic genes constituting the metabolic pathway (Usadel et al., 2009; Fukushima et al., 2011; Ginglinger et al., 2013). However, a coexpression analytical tool for *C. sinensis*, a nonmodel plant, is not yet available. For identification of the glucosyltransferases catalyzing the first glucosylation of volatiles, we surveyed UGTs coexpressing with structural genes for monoterpene biosynthesis in Arabidopsis by ATTED II (http://atted.jp), which is a database developed to identify functionally related genes by coexpression. By using the geraniol/nerol 10-hydroxylase gene (*At2g45580*; *CYP76C3*) and the linalool synthase gene (*At1g61680*; *AtLIS*; Mizutani et al., 1997; Obayashi et al., 2011; Ginglinger et al., 2013) as probes, we found that the expression profiles of Arabidopsis *UGT85A3* (At_UGT85A3, At1g22380; $r$ = 0.873) exhibit relatively high correlation with *AtLIS* and *CYP76C3* (Supplemental Fig. S1). In vitro functional characterization of At_UGT85A3 was performed using UDP-Glc as a sugar donor and geraniol or (*Z*)-3-hexenol as a sugar acceptor revealed that At_UGT85A3 produced geranyl-glc from geraniol and hexenyl-glc from (*Z*)-3-hexenol (Supplemental Figs. S2 and S3). These data demonstrate that At_UGT85A3 is capable of catalyzing the glucosylation of monoterpene alcohols and aliphatic alcohols.

### Identification of a *C. sinensis* UGT Catalyzing the First Glucosylation Step for Volatile β-Primeveroside

To isolate *C. sinensis* UGTs responsible for the first glucosylation step in volatile β-primeveroside biosynthesis, a complementary DNA (cDNA) library constructed from a mixture of leaves, stem, and roots of *C. sinensis* (Mizutani et al., 2002) was screened with digoxigenin (DIG)-labeled *At_UGT85A3*. Two rounds of screening

identified four novel UGTs, which were individually expressed in *Escherichia coli* and subjected to enzyme activity assays using UDP-Glc as a sugar donor and a variety of volatile alcohol acceptors. We found that one of the UGTs, named CsGT1, catalyzes the glucosylation of geraniol, as shown by the appearance of a product peak at the retention time of 10.2 min with mass-to-charge ratio 361 ($[M + HCOO]^-$), both values of which correspond to those of authentic geranyl-glc (Fig. 3, A and B). CsGT1 was assigned as Cs_UGT85K11 by the committee responsible for naming UDP-glucuronosyltransferases (Mackenzie et al., 1997).

The $V_{max}$ and estimated apparent $K_m$ values of CsGT1 for geraniol were 332.1 ± 8.1 nkat $mg^{-1}$ protein and 44.2 ± 3.0 μM, respectively (Table I). The sugar acceptor specificity of CsGT1 was surveyed using six aroma alcohols and two flavonoids found in tea leaves. CsGT1 was active toward all six volatiles with relative activities as follows: geraniol (100%), eugenol (84%), (*Z*)-3-hexenol (62%), benzyl alcohol (48%), 2-PE (9.2%), and linalool (1.4%); CsGT1 did not accept quercetin or cyanidine as substrates (Fig. 3C). On the other hand, CsGT1 showed clear preference to UDP-Glc (100%) as a sugar donor compared with UDP-Gal (15%), UDP-Xyl (not detected), and UDP-GlcA (not detected) when geraniol was used as a sugar acceptor (Fig. 3D). Taken together, these data indicate that CsGT1 preferentially glucosylates volatiles using UDP-Glc as a specific sugar donor but exhibits a broad substrate specificity for sugar acceptors.

### Identification of Orthologous UGTs of *CsGT1* from Various Plants

Volatile glycosides are reported in different plant species, including apricot (*Prunus armeniaca*), peach (*Prunus persica*), yellow plum (*Prunus domestica*; Krammer et al., 1991), grape (*Vitis vinifera*) berries (Günata et al., 1985), kiwi (*Actinidia chinensis*; Young and Paterson, 1995), strawberry (Roscher et al., 1996), raspberry (*Rubus* spp.; Pabst et al., 1991), and tomato (*Solanum lycopersicum*; Marlatt et al., 1992). Based on these general observations, we searched for UGTs in the National Center for Biotechnology Information GenBank (www.ncbi.nlm.nih.gov) based on amino acid sequence similarities with CsGT1 (accession no. AB847092). We found homologous UGTs broadly represented throughout the angiosperm plant lineages. We cloned another five UGTs from grapevine (Vv_UGT85A33, Vv_UGT85A28, Vv_UGT85A30), sweet potato (*Ipomoea batatas*; Ib_UGT85A32), and snapdragon (*Antirrhinum majus*; Am_UGT85A13) and experimentally characterized the recombinant enzymes by the procedure used for CsGT1. They exhibited volatile glycosylating activities similar to CsGT1, including the production of geranyl-glc and hexenyl-glc (Supplemental Figs. S2 and S3). These data show that UGTs with structural similarities, capable of catalyzing the first glucosylation step of aroma diglycosides such as β-primeverosides, are widely conserved in various plant lineages.

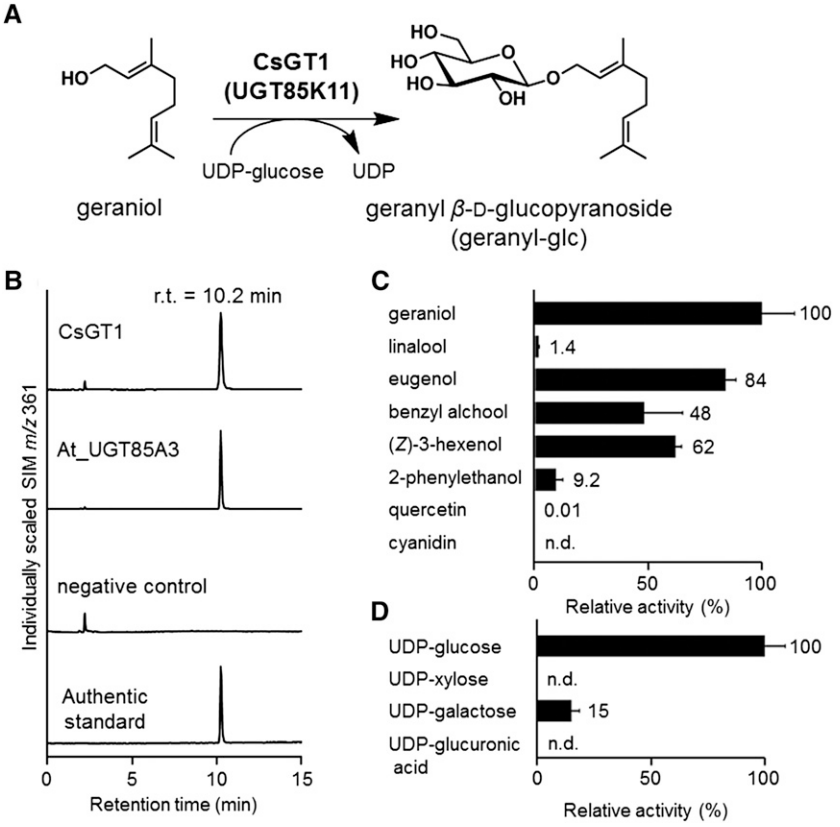


**Figure 3.** Biochemical characterization of CsGT1 and At_UGT85As. A, CsGT1 catalyzes the glucosylation of geraniol to produce geranyl-glc. B, LC-MS analysis of the enzymatic product of CsGT1 (UGT85K11) and At_UGT85A3 (At1g22380) compared with the authentic standard (geranyl-glu). n.d., Not detected; r.t., retention time; SIM, selected ion monitoring. C, Relative activity of CsGT1 toward sugar acceptors [geraniol, linalool, eugenol, benzyl alcohol, (*Z*)-3-hexenol, 2-PE, quercetin, and cyanidin]. D, Relative activity of CsGT1 toward sugar donors (UDP-Glc, UDP-Xyl, UDP-Gal, and UDP-GlcA). Data are presented as means ± SD ($n = 3$).

**Table I.** *Kinetic parameters of CsGT1 (UGT85K11) and CsGT2 (UGT94P1)*

Data are presented as means ± SD ($n$ = 3).

| Enzyme | Substrate | $K_m$ | $V_{max}$ | $V_{max}/K_m$ |
|---|---|---|---|---|
| | | $\mu M$ | *nkat* $g^{-1}$ *protein* | *nkat* $g^{-1}$ $\mu M^{-1}$ |
| CsGT1 (UGT85K11) | Geraniol | 44.2 ± 3.0 | 332.1 ± 8.1 | 7.5 ± 0.5 |
| CsGT2 (UGT94P1) | Geranyl β-D-glucopyranoside | 78.1 ± 19.6 | 60.0 ± 4.8 | 0.77 ± 0.2 |

### Purification of *C. sinensis* UGT Catalyzing the Second Xylosylation Step

To identify the UGT that is responsible for the second step (6-*O*-xylosylation for the Glc moiety of aroma monoglucoside), which is the conversion of aroma glucosides to aroma β-primeverosides, xylosyltransferase from young tea leaves was purified based on the xylosylation activity using geranyl-glc as a substrate at each step. The purification of the xylosyltransferase through seven purification steps resulted in 13-fold enrichment (Supplemental Table S2). Protein purity was assessed by SDS-PAGE followed by silver staining (Supplemental Fig. S4). Each excised protein band was subjected to LC-tandem mass spectrometry (MS/MS) to determine the partial amino acid sequence. De novo analysis (Peaks software; www.bioinfor.com) identified three peptide sequences (Supplemental Fig. S5A). Using the three peptide sequences (FPEVEKVELEEALPK, GLVVEGWAPQAR, and EEIEEIAHGLELSMVNFIWVVRFPEVEK) obtained from a single protein band, the corresponding cDNA was surveyed by a tBLASTn search in a *C. sinensis* EST database constructed by 454 GS-FLX (Roche; Ohgami et al., 2014). Contig134, encoding a partial UGT gene, was identified as the most likely candidate gene. A cDNA clone was isolated, carrying the sequence of contig134 in a 1,362-bp open reading frame, and encoded a polypeptide of 453 amino acid residues (calculated mass of 51.3 kD). The encoded polypeptide was named CsGT2, which was assigned as UGT94P1 by the committee responsible for naming UDP-glucuronosyltransferases (Mackenzie et al., 1997).

### Biochemical Characterization of the Xylosyltransferase

To test whether CsGT2 catalyzes the xylosylation of aroma glucosides into aroma β-primeverosides (Fig. 4A), we performed heterologous expression of CsGT2 in *E. coli* (Supplemental Fig. S6A) and in vitro enzymatic assays with recombinant CsGT2, using UDP-Xyl as a sugar donor and geranyl-glc as a sugar acceptor. Figure 4B shows that CsGT2 produced a new peak with a retention time at 4.9 min. This peak was identical to the authentic geranyl-pri, which was structurally determined to be xylosylated at the C-6′ position of the glucoside moiety by NMR spectroscopy (Guo et al., 1993). These results demonstrate that CsGT2 specifically catalyzes the xylosylation toward the C-6′ position of geranyl-glc. The $V_{max}$ and estimated apparent $K_m$ values of CsGT2 were

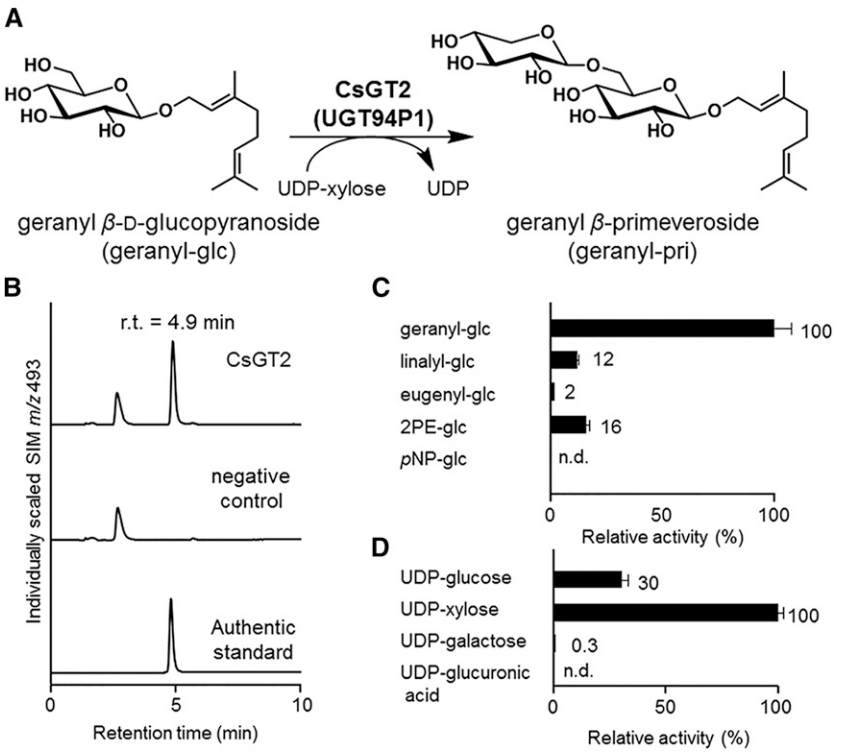


**Figure 4.** Biochemical characterization of CsGT2. A, CsGT2 (UGT94P1) catalyzes the xylosylation of geranyl-glc into geranyl β-primeveroside. B, LC-MS analysis of the enzymatic product of CsGT2 (UGT94P1) compared with an authentic standard (geranyl-pri; retention time [r.t.] = 4.9 min). n.d., Not detected; SIM, selected ion monitoring. C, Relative activity of CsGT2 toward sugar acceptors (geranyl-glc, linalyl-glc, eugenyl-glc, 2PE-glc, and *p*NP-glc). D, Relative activity of CsGT2 toward sugar donors (UDP-Glc, UDP-Xyl, UDP-Gal, and UDP-GlcA).

determined to be 60.0 ± 4.8 nkat $mg^{-1}$ protein and 78.1 ± 19.6 μM, respectively (Table I). The substrate specificity of CsGT2 was determined using four aroma glucosides and one nonnatural glucoside as sugar acceptors. CsGT2 was active toward all four aroma glucosides with the following relative activities: geranyl-glc (100%), 2PE-glc (16%), linalyl-glc (12%), and eugenyl-glc (2%), but not toward the nonnatural *p*-nitrophenyl β-D-glucopyranoside (*p*NP-glc; Fig. 4C). It is important to mention that CsGT2 did not exhibit any activity toward monoterpene alcohols (volatile aglycones).

On the other hand, investigation of the specificity of CsGT2 toward various sugar donors using geranyl-glc as a sugar acceptor revealed that CsGT2 preferentially used UDP-Xyl (100%) as a sugar donor, while a weak activity was detected with UDP-Glc (30%) and no apparent activity was found for UDP-GlcA or UDP-Gal (Fig. 4D). These results demonstrate that CsGT2 preferentially catalyzes the xylosylation of aroma glucosides, leading to the formation of aroma β-primeverosides.

### Homology Modeling and Mutagenesis Analysis of CsGT2

The sugar donor specificity of UGTs is dictated by a small number of amino acid residues (Osmani et al., 2008; Noguchi et al., 2009; Ono et al., 2010a). The residues are located in three distinct domains: N-terminal, middle, and C-terminal (PSPG box) domains (Sayama et al., 2012). To gain insights into the molecular mechanism of the UDP-Xyl specificity of CsGT2, we constructed a structural model of CsGT2 by homology modeling (Discovery Studio 3.5 [DS3.5]; Accelrys). The crystal structures of the glycosyltransferases, At_UGT72B1 (Protein Data Bank [PDB] code 2vce) and Mt_UGT85H2 (PDB code 2pq6), were selected as templates for their similarities to CsGT2. In addition, we used the three-dimensional (3D) structure of the sugar donor, UDP-2F-Glc, and the crystal structure of grape UDP-Glc: flavonoid 3-*O*-glycosyltransferase VvGT1 (PDB code 2c1z; Offen et al., 2006). In the constructed homology model, Ile-141 was identified as a candidate residue for the control of sugar donor specificity because it is located proximal to UDP-Xyl (Fig. 5, A and E). This unique Ile-141 was found to be conserved in two xylosyltransferases specific for flavonoid glycosides, kiwi F3GGT1 (Ile-136) and Arabidopsis UGT79B1 (Ile-142; Montefiori et al., 2011; Yonekura-Sakakibara et al., 2012; Table II). In contrast, various amino acid residues occupy this position in other structurally similar glycosyltransferases, including morning glory (*Ipomoea purpurea*) UGT79G16 (Thr-138), *Sesamum indicum* UGT94D1 (Ser-140), *Veronica persica* UGT94F1 (Ala-144), and tomato NONSMOKY GLYCOSYLTRANSFERASE1 (Sl_NSGT1 [Val-145]; Table II; Morita et al., 2005; Noguchi et al., 2008; Ono et al., 2010b; Tikunov et al., 2013). To assess the functional relevance of Ile-141 for the specificity toward UDP-Xyl, a CsGT2-I141S mutant was generated by site-specific mutagenesis, in which Ile-141 was replaced by a Ser residue. CsGT2-I141S was heterologously expressed in *E. coli* (Supplemental Fig. S6B). Compared with wild-type CsGT2, the mutant exhibited significantly lower activity with UDP-Xyl but higher activity with UDP-Glc (Fig. 5, C and D). These experiments identified Ile-141 as the crucial residue responsible for the sugar donor specificity of CsGT2 for UDP-Xyl.

### Gene Expression and Phylogenetic Analysis of CsGT1 and CsGT2

The tissue specificity of the glycosylation of volatiles was assessed by quantitative real-time (qRT)-PCR performed with specific organs of *C. sinensis* (leaves from young to fully mature stage, stems, roots, and flowers). Both *CsGT1* and *CsGT2* were highly expressed in young leaves, where *β-PD* was also found to be highly expressed (Fig. 6). During leaf maturation, the expression of *CsGT1* and *CsGT2* decreased, which is consistent with the accumulation profile of β-primeverosides (Fig. 2).

Sequence analysis indicated that CsGT1 and CsGT2 only share 27% amino acid identity. Phylogenetic analysis showed that CsGT1 and CsGT2 belong to different clades, OG2 and OG8, respectively (Yonekura-Sakakibara and Hanada, 2011; Fig. 7). CsGT1 showed high similarity to cassava (*Manihot esculenta*) UGT85K4 and UGT85K5 involved in the biosynthesis of cyanogenic glucosides (Kannangara et al., 2011). In contrast, CsGT2 constitutes a new member of the so-called sugar-sugar UGT or glycoside-specific glycosyltransferase (GGT) group that specifically catalyzes glycosylation at the sugar moiety of various phytochemical glycosides (but not aglycones), including the morning glory DUSKY (UGT79G16) and tomato NSGT1 involved in the glucosylation of anthocyanin and volatile glycosides, respectively (Morita et al., 2005; Tikunov et al., 2013).

### Tissue Localization of a Selected Aroma Glycosidic Precursor

The preferential expression of the two *CsGTs* in young leaves is consistent with the accumulation of β-primeverosides in plant tissue (Fig. 2). To gain further insights into the biological role of aroma glucosides and aroma β-primeverosides, mass spectrometry imaging analysis was conducted to localize the metabolites in the young leaves at the cellular level. The specific signals, with mass-to-charge ratios of 417, 284, and 340 corresponding to hexenyl-pri, hexenyl-glc, and geranyl-glc, respectively, were preferentially detected in the epidermal layer of tea leaves, indicating a highly regulated distribution of the aroma glycosidic precursor (Supplemental Fig. S7).

## DISCUSSION

### CsGT1 and CsGT2 Catalyze the Two Glycosylation Steps of Volatile Monoterpenes and Alcohols

The broad substrate specificity of CsGT1 for sugar acceptors substantiates the structural diversity of the β-primeverosides of monoterpenes and primary alcohols known to accumulate in tea leaves (Fig. 2). CsGT1

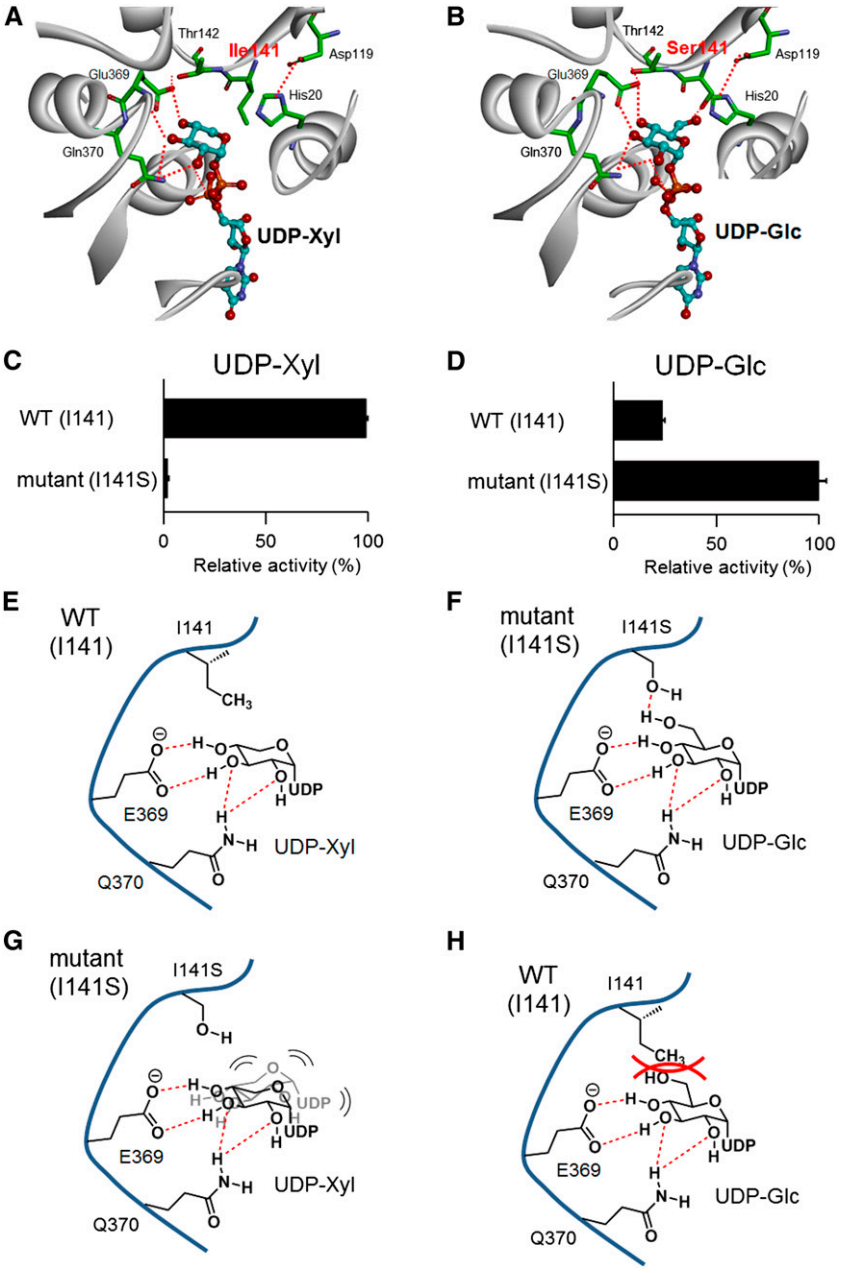


**Figure 5.** Structural comparison of the sugar-donor specificity of CsGT2 and its mutant, CsGT2 (I141S). A, Homology model of UDP-Xyl-bound CsGT2. B, Homology model of UDP-Glc-bound CsGT2 (I141S). For the homology models, important amino acid residues on the active site are drawn as the stick form and UDP sugars as the ball-and-stick form. Carbon atoms are colored in green for UGT amino acid residues and in cyan for UDP sugars. Oxygen atoms are red, nitrogen atoms are blue, and phosphorus atoms are orange. Plausible hydrogen bonds are indicated by the red dotted lines. To simplify the visibility of the models, the structure of a sugar acceptor is removed. C, Relative activity of wild-type CsGT2 (WT) and CsGT2 (I141S) toward UDP-Xyl with geranyl-glc as a sugar acceptor. D, Relative activity of wild-type CsGT2 and CsGT2 (I141S) toward UDP-Glc with geranyl-glc as a sugar acceptor. Data are presented as means ± SD ($n$ = 3). E, Schematic representation of UDP sugar recognition of wild-type CsGT2 and UDP-Xyl (schematic model in A). F, Schematic representation of UDP sugar recognition of CsGT2 (I141S) and UDP-Glc (schematic model in B). G, Schematic representation of UDP sugar recognition of CsGT2 (I141S) and UDP-Xyl. H, Schematic representation of UDP sugar recognition of wild-type CsGT2 and UDP-Glc.

belongs to the UGT85 family and shows similarities in structure and function to kiwi AdGT4 and grape VvGT14, VvGT16, VvGT17, and VvGT19 that were recently shown to catalyze the glucosylation of small terpenes and primary alcohols that are accumulated as glycosides in ripe kiwi and grape (Bönisch et al., 2014a, 2014b; Yauk et al., 2014). It is noteworthy that AdGT4, VvGT14, and VvGT16 also have broad substrate specificities toward volatile sugar acceptors (Bönisch et al., 2014a; Yauk et al., 2014). Taken together, our data and these studies support the notion that the machinery behind the glucosylation of monoterpenes and primary alcohols is fairly conserved among phylogenetically discrete various plant species (tea plant, kiwi, grapevine, Arabidopsis, snapdragon, and sweet potato; Supplemental Figs. S2 and S3; Bönisch et al., 2014a; Yauk et al., 2014). The estimated apparent $K_m$ of CsGT1 for geraniol (44 $\mu$M) was comparable to those of other volatile UGTs isolated from kiwi and grape [AdGT4 for (Z)-3-hexenol, 57 $\mu$M; VvGt14, VvGT15a, VvGT15b, VvGT15c, and VvGT16 for citronellol, 9, 29, 55, 20, and 108 $\mu$M, respectively]. These UGTs were found to be highly expressed in young tea leaves, ripe kiwi, and grape, where aroma glucosides are dominantly accumulated. Furthermore, the concentrations of substrates, (Z)-3-hexenol in ripe kiwi, citronellol in grape, and geraniol in young tea leaves, were determined to be at least 0.8, 1.0, and 5.8 mM, respectively (Bönisch et al., 2014a; Yauk et al., 2014). Their relatively lower substrate specificity toward volatile sugar acceptors, compared with those of previously characterized nonvolatile UGTs, might

**Table II.** *Comparison of the substrate specificity of GGTs in the OG8 cluster*

Bold type indicates the positions of Ile-141 of CsGT2 and corresponding amino acid residues of GGTs in the OG8 cluster with UDP-Xyl as the sugar donor.

| GGT (OG8) | Species | Substrate Specificity | | | Sequence Alignment |
|---|---|---|---|---|---|
| | | Sugar Donor | Sugar Acceptor | Position | |
| CsGT2 (UGT94P1) | Tea | **UDP-Xyl** | Volatile glucoside | 6′ | IPAVQLM**I**TGAT **141** |
| AcF3GGT1 | Kiwifruit | **UDP-Xyl** | Flavonoid galactoside | 2′ | IKSVNYC**I**ISPA **136** |
| UGT79B1 | Arabidopsis | **UDP-Xyl** | Flavonoid glucoside | 2′ | AKTVCFN**I**VSAA **142** |
| UGT79B6 | Arabidopsis | UDP-Glc | Flavonoid glucoside | 2′ | VKSVNFI**T**ISAA **135** |
| UGT94D1 | *S. indicum* | UDP-Glc | Lignan glucoside | 6′ | IPAMVFL**S**TGAA **140** |
| UGT94F1 | *V. persica* | UDP-Glc | Flavonoid glucoside | 2′ | SPSVWFM**A**SGAT **144** |
| DUSKY (UGT79G16) | Morning glory | UDP-Glc | Flavonoid glucoside | 2′ | IKSVFYS**T**ISPL **138** |
| NSGT1 | Tomato | UDP-Glc | Volatile glycoside | 2′ | IHAIMFY**V**SSTS **145** |

reflect their promiscuous biochemical nature, recognizing structurally diverse substrates. Taken together, UGT85-related enzymes play a role in the formation of aroma glucosides in various plants.

On the other hand, CsGT2 was identified as a novel UGT that specifically catalyzes the 6-*O*-xylosylation of the sugar moiety of aroma monoglucosides, the second step of glycosylation in the biosynthesis of β-primeverosides (Fig. 4A). CsGT2 belongs to the GGT cluster (OG8), with regio-specificity for the C-2 hydroxy or C-6 hydroxy group of sugar moieties of various phytochemical glycosides (Noguchi et al., 2008). CsGT2 is phylogenetically related to tomato NSGT1, which catalyzes the third 2-*O*-glucosylation of volatile-derived diglycosides (Tikunov et al., 2013; Fig. 7). The majority of UGTs within this GGT cluster catalyze the sugar-sugar glycosylation of various phytochemicals, such as flavonoids, triterpenoids, and lignans (Morita et al., 2005; Sawada et al., 2005; Noguchi et al., 2008; Shibuya et al., 2010; Yonekura-Sakakibara et al., 2014). Therefore, it is conceivable that an ancestral GGT has adapted to accommodate structurally diverse specialized metabolites that often exist only in particular plant lineages while maintaining its unique regio-specificity for the sugar moiety. The biochemical activities of CsGT1 and CsGT2 suggest their participation in the biosynthesis of aroma β-primeverosides in tea plants.

### *Sugar Donor Specificity of CsGT2 for UDP-Xyl*

UGTs usually show exclusive sugar donor specificity, which is determined by a small number of amino acid residues proximal to the bound sugar donor in the substrate-binding pocket (Osmani et al., 2008; Noguchi et al., 2009; Ono et al., 2010a). These crucial residues for sugar donor specificity are located in three distinguishable regions, the N-terminal, middle, and C-terminal regions (Sayama et al., 2012). Mutagenesis experiments (Ile-141→Ser-141) revealed that the unique Ile-141 of CsGT2 located in the middle region is a residue determining the specificity toward UDP-Xyl. The fact that the CsGT2-I141S mutant had considerably higher specificity for UDP-Glc supports the notion that the xylosyltransferase evolved from a glucosyltransferase by the acquisition of the crucial Ile-141. It should be noted that an Ile residue, which corresponds to Ile-141 in CsGT2, is also present in the midregion of the two flavonoid 3-*O*-glycoside:2′′-*O*-xylosyltransferases (kiwi Ac_F3GGT1 and Arabidopsis UGT79B1) but not in Arabidopsis flavonol 3-*O*-glucoside:2′′-*O*-glucosyltransferase (UGT79B6; Table II; Yonekura-Sakakibara et al., 2012, 2014). These data suggest that the recognition mechanism for UDP-Xyl by CsGT2 is similar to those of xylosyltransferases

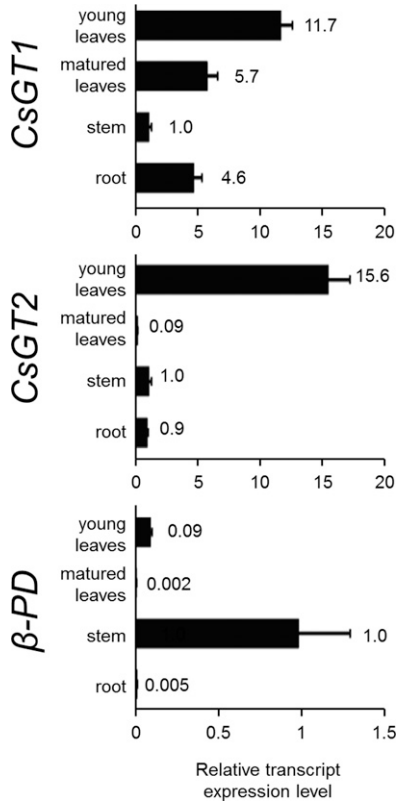


**Figure 6.** Relative transcript abundance of *CsGT1*, *CsGT2*, and *β-PD* in various organs (young leaves, mature leaves, stem, root, and flower) of *C. sinensis*. Transcript abundance was measured by qRT-PCR and normalized to the internal reference 18S ribosomal RNA (*18S rRNA*). The expression level of each gene in the stem was set at 1. Data are presented as means ± SD ($n = 3$).

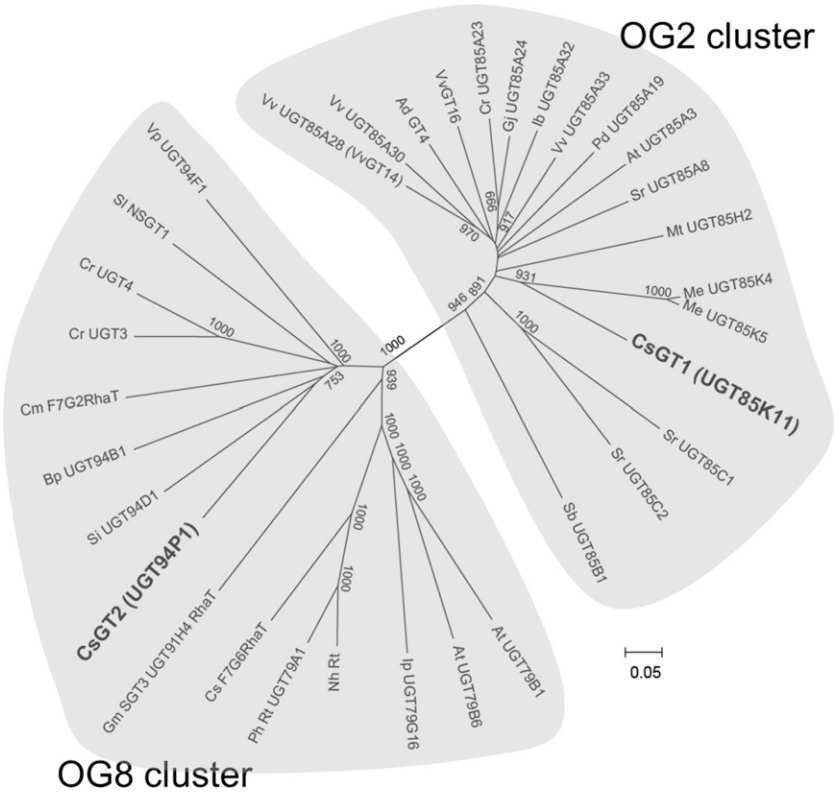


**Figure 7.** Phylogeny of the UGT-glucosyltransferase OG2 and OG8 family. All other UGT sequences were available for Arabidopsis on The Arabidopsis Information Resource Web site. High bootstrap values (greater than 750) are indicated on the branches (1,000 replicates). The Vv_UGT85A28 described here was found to be identical to VvGT14 (Bönisch et al., 2014b).

from kiwifruit and Arabidopsis, although these two UGTs specifically recognize flavonoid glycosides as their sugar acceptors.

The hydrophobic bulky side chain of the Ile residue possibly contributes to the unique sugar donor specificity of CsGT2 for UDP-Xyl by hindering the access of sugar donors with a functional group at the C6 position (UDP-Glc, UDP-Gal, and UDP-GlcA) to the substrate pocket of GGT xylosyltransferases. In contrast, the CsGT2-I141S mutant showed a preference for UDP-Glc instead of UDP-Xyl as a sugar donor (Fig. 5, C and D). Therefore, the hydroxy group of Ser-141 could contribute to the recognition of UDP-Glc via a hydrogen bond with the C6 hydroxy group of UDP-Glc (Fig. 5, B and F). Conversely, the fact that the CsGT2-I141S mutant failed to use UDP-Xyl as a sugar donor suggests that the hydroxy group of the side chain of Ser-141 prevents binding to UDP-Xyl because of a lack of the C6 functional group in the sugar donor-binding pocket, probably via hydrophilic properties. The bulky side chain of the Ile may structurally be required to form an appropriate sugar donor-binding pocket for UDP-Xyl (Fig. 5, G and H).

Soybean (*Glycine max*) Sg-1[a] (Gm_UGT73F4) of the OG1 cluster is a xylosyltransferase involved in the biosynthesis of triterpenoid soyasaponins but has no Ile residue corresponding to Ile-141 of CsGT2. Instead, Sg-1[a] has a unique Ser residue (Ser-138) in the middle domain found to be essential for its sugar donor specificity toward UDP-Xyl (Sayama et al., 2012). Therefore, our findings indicate that the typical sugar donor specificity of CsGT2 and Sg-1[a] for UDP-Xyl results from convergent evolution, because (1) Sg-1[a] and CsGT2 are phylogenetically remote GGTs specialized for structurally different substrates (glycosides of large triterpenes versus small volatile monoterpenes, respectively) but with the same sugar donor specificity for UDP-Xyl, and (2) replacement of Ile-141 with a Ser residue in the CsGT2-I141S mutant resulted in a significant decrease in specificity for UDP-Xyl (Fig. 5C), whereas replacement of Ser-138 with Gly in Sg-1[a] (S138G) converted the xylosylating activity into a glucosylating activity (Sayama et al., 2012). These findings not only highlight the plasticity of the sugar donor specificity of UGTs but demonstrate that the metabolic specialization is a consequence of the lineage-specific differentiation of the enzymes.

### *Putative Physiological Roles of CsGT1 and CsGT2 in Volatile Metabolism*

The predominant gene expression of the two *CsGTs* into young tea leaves, together with the localization of geranyl-pri, 2PE-pri, and hexenyl-pri in the same organ, suggest that these VOCs play physiological roles in this tissue. Given that VOCs are chemical defense precursors against fungi and herbivores, CsGTs and $\beta$-PD play vital roles in the storage and release of *C. sinensis* VOCs, respectively. Based on these data, we propose a plausible volatile metabolism in the tea plant where tissue damage caused by herbivores would allow geranyl-pri to encounter extracellular $\beta$-PD, resulting in the rapid release of geraniol into the air, without de novo biosynthesis (Fig. 8). It is of particular interest to reveal the

sophisticated defense system and whether the molecular evolution of the second enzyme, CsGT2, is coupled to the evolution of β-PD, which specifically hydrolyzes diglycosides but is inactive against monoglycosides (Mizutani et al., 2002).

Linalyl-pri dominantly accumulated in stems, while geranyl-pri accumulated in leaves (Fig. 2). However, CsGT1 exhibited less activity toward linalool compared with geraniol, while CsGT2 showed weaker activity for linalyl-glc than geranyl-glc. Moreover, both CsGT1 and CsGT2 were predominantly expressed in young leaves rather than stem (Fig. 6). These data suggest that geraniol and linalool are separately biosynthesized in leaves and stems of tea plants, respectively, and that members of an unknown class of glucosyltransferases specifically catalyze the glucosylation of linalool and linalyl-glc. This notion is supported by recent reports that kiwi AdGT4 and grape VvGT14, which are UGT85-class glucosyltransferases for volatiles, also showed little enzyme activity toward linalool, in contrast to their preferred substrate, geraniol (Bönisch et al., 2014b; Yauk et al., 2014). Since CsGT1, AdGT4, and VvGT14 commonly exhibited substrate preference to the primary alcohols geraniol and (*Z*)-3-hexenol over the tertiary alcohol linalool, there might be a structural feature of substrate recognition that is shared by these enzymes. Together, these data suggest the possibility that the molecular machinery for volatile glycosides could be distinct in leaves and stems of the tea plant.

Various plant species use the glycosylation of specialized metabolites to increase their solubility, which constitutes a primary strategy to accumulate metabolites operating as defensive compounds against herbivores and pathogens. At the same time, glycosylation of the metabolites facilitates the transport of the resulting glycosides to specific compartments, where they are stored separately from hydrolyzing enzyme glycosidases. For instance, tissue damage by insect attack or pathogen infection triggers the production of the phytotoxin 2,4-dihydroxy-7-methoxy-1,4-benzoxazin-3-one (DIMBOA) by a β-glucosidase that hydrolyzes the stored form 2-(2,4-dihydroxy-7-methoxy-1,4-benzoxazin-3-one)-β-D-glucopyranoside (DIMBOA-glucoside; Frey et al., 2009). Similarly, glucosinolates (β-thioglucoside-*N*-hydroxysulfates) are precursors of the isothiocyanates and nitriles known as mustard oil bomb against insects. These glucosinolates are compartmentalized into a glucosinolate-rich cell type (S-cells), whereas the myrosinases that hydrolyze glucosinolates are only expressed in myrosin cells (Koroleva et al., 2010). Tissue damage by insects elicits the hydrolysis of glucosinolates by myrosinases and the accumulation of isothiocyanates and nitriles.

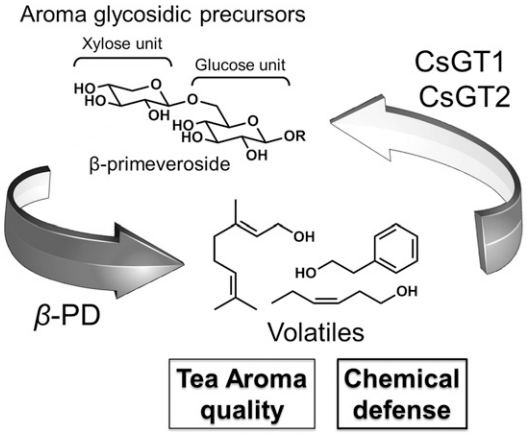


**Figure 8.** Schematic illustration of a mode of action of CsGT1, CsGT2, and β-PD in the volatile metabolism in *C. sinensis*.

On the other hand, volatile alcohols and monoterpenes are mainly stored in the form of diglycosides. Interestingly, various sugars (i.e. Xyl, Ara, apiose, and Rha) could be attached to monoglycosides of VOCs as second sugar molecules (Tikunov et al., 2013; Bönisch et al., 2014b). This observation suggests that the second sugar moiety of the glycoconjugated VOCs further increases stability, which leads to the accumulation of such glycoconjugated VOCs. Calculation of the cLogP (low value indicates high water solubility) revealed that the two sequential glycosylation reactions supporting the conversion of geraniol into geranyl-pri are associated with a stepwise increase in hydrophilicity, from 2.97 to 2.00 (geranyl-glc) and from 2.00 to 0.46 (geranyl-pri). The cLogP value significantly depends on the sugar type at the nonreducing end as well as the sugar number (Tsukada et al., 2006). Furthermore, the existence of exoglycosidases that cleave disaccharide primeverose into Glc and Xyl has not been established in tea plant or other plants. Therefore, the xylosylation of geranyl-glc by CsGT2 shown in this study should substantially contribute to the increase in water solubility and the endurance against exoglycosidases. In addition, the increase in water solubility of geraniol through glycosylation may be related to the fact that geraniol and other monoterpene alcohols exhibit high apoptosis-inducing activity in plant cells (Izumi et al., 1999). This toxic nature of geraniol necessitates precise control of its biosynthesis and conversion into monoglycosides and diglycosides by CsGT1 and CsGT2, respectively, for the accumulation of defensive geranyl-pri upon potential attacks by herbivores.

## CONCLUSION

β-Primeverosides are the most abundant form of aroma diglycosides in *C. sinensis*, and they are commercially and physiologically important for tea aroma quality in dietary beverages and for chemical defense against herbivores in the tea plant. Here, we demonstrated through metabolic profiling of aroma glycosides in the plant, enzymatic characterization, and transcript analysis that CsGT1 and CsGT2 catalyze the sequential glucosylation and xylosylation of aromas, respectively, leading to the production of aroma β-primeverosides. The transcripts of the two *CsGTs* and *β-PD* in young tea leaves, together with the localization of geranyl-pri in

epidermal cells of young tea leaves, strongly support the potent physiological role of VOCs in chemical defense primarily in this tender tissue. Here, we report the identification and characterization of molecular machineries for the biosynthesis of β-primeverosides of tea aroma. Our findings provided not only molecular insights into volatile metabolism in *C. sinensis* but also crucial molecular tools for controlling tea aroma quality and for understanding of a sophisticated chemical defense system elaborated during plant evolution.

## MATERIALS AND METHODS

### Chemicals

*p*NP-pri, eugenyl-pri, and 2PE-pri were kindly provided by T. Usui and T. Murata (Shizuoka University; Murata et al., 1999). Geranyl-pri and linalyl-pri were prepared as described (Guo et al., 1993, 1994). *p*NP-glc, cyanidin 3-*O*-glucoside chloride, and quercetin 3-*O*-glucoside were purchased from Sigma-Aldrich (www.sigmaaldrich.com). Other glucosides were chemically synthesized using the procedure for 2PE-glc as described previously (Ma et al., 2001). UDP-Xyl was obtained from CarboSource Services at the University of Georgia. Other chemicals were purchased from Sigma-Aldrich and Wako Pure Chemical Industries (www.wako-chem.co.jp/english/).

### Plant Materials

Young leaves of tea plant (*Camellia sinensis* var *sinensis* 'Yabukita') were harvested at the Center for Education and Research of Field Sciences, Shizuoka University, and at the Tea Research Center, Shizuoka Prefectural Research Institute of Agriculture and Forestry. The young and mature developmental stages of leaves and stems were defined as follows: young leaves, which are the first, second, and third leaves (plucking part for high-grade tea products); mature leaves, which are the fourth and fifth leaves; stem, which is the green young nonlignified part between the third and fifth leaves; and branch, which is the brown lignified old part (Supplemental Fig. S8). All plant materials were quickly frozen in liquid nitrogen and stored at −80°C prior to use.

### Quantification of Endogenous Aroma Glycosides in *C. sinensis*

A total of 3.5 g (fresh weight) of leaves and stems at two developmental stages (young and mature) of *C. sinensis* was finely crushed in a tissue mill (TK-AM5; Taitec; www.e-taitec.com), suspended in 80% (v/v) methanol (30 mL), and filtrated. The filtrate was concentrated in vacuo and separated with *n*-hexane. The aqueous layer was concentrated in vacuo, dissolved in distilled water, and purified with Oasis HLB (3 cc; Waters; www.waters.com). The glycosidic fractions were concentrated in vacuo and dissolved in distilled water prior to LC-MS analysis. Detailed procedures for LC-MS analysis are given in Supplemental Materials and Methods S1.

### Identification of *CsGT1*

A full-length cDNA clone of *CsGT1* was isolated by a screen with full-length DIG-labeled mixed probes for At_UGT85A in a cDNA library derived from *C. sinensis* described previously (Mizutani et al., 2002). Library screening was performed under a low-stringency condition as described by Yonekura-Sakakibara et al. (2000) and Noguchi et al. (2008, 2009). The screening probes of At_UGT85A were DIG labeled by PCR using gene-specific oligonucleotides (Supplemental Table S3). More than 50 positive clones were obtained in approximately 5,000,000 plaques after two rounds of screening. The cDNA fragments of positive clones were sequenced by a conventional primer-walking method with the BigDye-terminator version 3.1 cycle sequencing kit (Life Technologies; www.lifetechnologies.com). Among these clones, a full-length cDNA for the *CsGT1* gene was identified by BLASTx search based on sequence similarities with At_UGT85A3.

### Enzyme Purification of a Xylosyltransferase Specific for Monoglucoside-Bound Volatiles

All procedures were performed at 4°C. The compositions of the purification buffers and solutions for peptide analysis are described in Supplemental Table S4. Tea leaves (100 g) were finely chopped, crushed in a tissue mill (Taitec), suspended in 100 mL of buffer A, and centrifuged (20,000*g*, 30 min). The supernatant was collected, and ammonium sulfate was added to 30% saturation. The mixture was centrifuged (20,000*g*, 30 min), the supernatant was collected, and ammonium sulfate was added up to 70% saturation, followed by another centrifugation (20,000*g*, 30 min). The pellet was dissolved in buffer B and dialyzed against buffer B for complete removal of the ammonium sulfate. Purification **of** active fractions was performed using the following columns: HiTrap DEAE FF (5 mL; GE Healthcare; www.gelifesciences.com), HiTrap Q FF (5 mL), Macro-prep Ceramic Hydroxyapatite Type III (5 mL; Bio-Rad; www.bio-rad.com), HiTrap Blue HP (1 mL), and Mono Q 5/50 GL (1 mL). At each purification step, the eluted fractions were tested for xylosyltransferase activity toward geranyl-glc by LC-MS, and the active fractions were pooled before the next purification step. Detailed procedures are given in Supplemental Materials and Methods S1.

### Identification of the Peptide Sequence of CsGT2 by LC-MS/MS

Purified proteins were separated by SDS-PAGE and stained by silver staining, and the major bands were excised from the gel and destained with solution F. Proteins in the gel pieces were reduced and alkylated in solutions G and H, respectively, followed by solution H. After serial washes with wash solution F and acetonitrile, the proteins were digested with trypsin (Promega; www.promega.com). The tryptic peptides were extracted from the gel pieces with solution I, and the extract was concentrated in vacuo. The concentrated solution was centrifuged (20,000*g*, 10 min), and the supernatant was analyzed by LC-MS/MS (Supplemental Materials and Methods S1). All peptide mass data were analyzed using Peaks software (Bioinformatics Solutions).

### Identification of Full-Length *CsGT2* cDNA

Since contig134 had a partial open reading frame of *CsGT2*, the full-length sequence of *CsGT2* cDNA was obtained from fresh young tea leaves using gene-specific CsGT2-Race-FW and CsGT2-Race-RV oligonucleotides, using the SMARTer cDNA RACE cDNA amplification kit (Clontech; www.clontech.com) and PrimeStar HS polymerase (Takara Bio; www.takara-bio.com), according to each manufacturer's instructions. The amplified products were gel purified and ligated into pJET 1.2 vector using the CloneJET kit (Thermo Fisher Scientific; www.thermoscientificbio.com).

### Heterologous Expression of Recombinant UGT Proteins

Total RNA was extracted from fresh young tea leaves using the RNeasy Plant Mini kit (Qiagen; www.qiagen.com), according to the manufacturer's instructions. cDNA was reverse transcribed from 1 μg of total RNA with SuperScript III (Life Technologies). Full-length cDNA fragments of *CsGT1* and *CsGT2* genes were amplified from cDNA of cv Yabukita by reverse transcription-PCR using gene-specific oligonucleotides (Supplemental Table S3). In vitro mutagenesis of the *CsGT2* gene was performed by recombinant PCR with specific mutagenic oligonucleotides (Supplemental Table S3) as described previously (Noguchi et al., 2009). For their expression in *Escherichia coli*, the generated amplicons were ligated into the pENTR/D-TOPO vector (Life Technologies), and the sequence was verified. They were subcloned into the pET15b expression vector (Merck Millipore; www.merckmillipore.com) and transformed into *E. coli* BL21 (DE3; Toyobo; www.toyobo-global.com). The recombinant proteins produced by *E. coli* BL21 were quantified by the method of Bradford (1976) with bovine serum albumin as the standard and separated by SDS-PAGE. The expressed recombinant proteins were immunologically detected on the gels by western blotting as described previously (Sayama et al., 2012).

### Enzyme Assay of CsGT1 and CsGT2

For relative activity assays of CsGT1 and CsGT2, the enzymatic reaction mixture (50 μL) consisted of 100 mM sugar acceptor, 2 mM sugar donor, 50 mM potassium phosphate buffer, pH 8, and enzyme. The enzyme assays were initiated after preincubation of the mixture without the enzyme at 30°C for 5 min.

After incubation at 30°C for 10 min, the reaction was stopped by the addition of 50 μL of ice-cold methanol. The same assay conditions were used for determination of the kinetic parameters of CsGT1 and CsGT2, except that the sugar acceptor geranyl-glc was used instead of geraniol and at six different concentrations from 1.25 to 250 μM. The enzymatic products were analyzed by LC-MS analysis (Supplemental Materials and Methods S1). The apparent $K_m$ and $V_{max}$ values for each sugar donor and the sugar acceptor (geraniol) were determined at a saturating substrate concentration by fitting the initial linear velocity data to a Michaelis-Menten equation using nonlinear regression analysis in the Kaleidagraph software (www.synergy.com).

## Homology Modeling

The construction of a 3D model according to CsGT2 was conducted using DS3.5 (Accelrys; http://accelrys.com/). The crystal structures of At_UGT72B1 (PDB code 2vce), Mt_UGT85H2 (PDB code 2pq6), and VvGT1 (PDB code 2c1z) and the 3D structure of the sugar donor UDP-2-F-Glc were used as templates. The initial structure of CsGT2 was constructed using the multiple homology modeling protocols of the DS3.5 Modeler module. The resulting CsGT2 structure was inserted in the UDP-2F-Glc bound in VvGT1, and the sugar moiety of UDP-2F-Glc was replaced with a Xyl. Structure optimization of the initial complex model (CsGT2-UDP-Xyl) was performed using molecular mechanics and dynamics simulation with the CHARMm force field of DS3.5. On the other hand, the 3D structure of the CsGT2 (I141S) mutant was first constructed by replacing Ile-141 with a Ser residue. After insertion of UDP-2F-Glc bound to VvGT1, the fluoride atom of UDP-2F-Glc was converted to a hydroxy group to generate the model complex, CsGT2 (I141S)-UDP-Glc, which was optimized by the same procedure used for CsGT2-UDP-Xyl.

## qRT-PCR of *CsGTs* and *β-PD*

qRT-PCR was performed as described previously (Noguchi et al., 2008). In brief, the cDNA was prepared from multiple organs and tissues of *C. sinensis*. The *CsGT1*, *CsGT2*, *β-PD*, and *18S rRNA* were quantified by real-time PCR using specific primers (Supplemental Table S3) and the Power SYBR Green PCR kit (Qiagen) on the 7500 Real-Time PCR system (Life Technologies). The transcription levels were quantified using the ΔΔ*Ct* threshold cycle method (Life Technologies) and normalized to the expression level of an internal standard (*18S rRNA*). The results are presented as means ± SE of three independent experiments.

## Phylogenetic Analysis

The amino acid sequences of UGTs (Supplemental Fig. S9; Supplemental Table S5) were aligned based on codon position using ClustalW bundled in MEGA6 (Tamura et al., 2013). All sites containing gaps and missing data were eliminated from the remaining analysis. Unrooted phylogenetic trees were reconstructed by neighbor-joining methods from the translated amino acid sequences. The neighbor-joining tree was reconstructed by MEGA6, and the matrix of evolutionary distances was calculated by Poisson correction for multiple substitutions. The reliability of the reconstructed tree was evaluated by a bootstrap test for 1,000 replicates.

Sequence data from this article can be found in GenBank/EMBL under the following accession numbers: UGT85K11 (AB847092) and UGT94P1 (AB847093).

## Supplemental Data

The following supplemental materials are available.

**Supplemental Figure S1.** Coexpression analysis of *AtLIS*, *CYP76C3*, and *UGT85A3* by ATTED II (gene coexpression database; http://atted.jp/) version C4.1.

**Supplemental Figure S2.** Enzymatic activity of CsGT1 homologs for (*Z*)-3-hexenol.

**Supplemental Figure S3.** Enzymatic activity of CsGT1 homologs for geraniol.

**Supplemental Figure S4.** Purified enzymes catalyzing the second xylosyltransferase (CsGT2).

**Supplemental Figure S5.** Partial peptide sequence of CsGT2.

**Supplemental Figure S6.** Recombinant proteins of a series of CsGTs.

**Supplemental Figure S7.** Mass spectrometry imaging of young fresh leaves of *C. sinensis*.

**Supplemental Figure S8.** Harvesting individual tissues for the quantification of endogenous aroma glycosides and qRT-PCR of *CsGT1*, *CsGT2*, and *β-PD*.

**Supplemental Figure S9.** Multiple sequence alignment of protein sequences of the UGT-glucosyltransferase OG2 and OG8 family.

**Supplemental Table S1.** Summary of fresh weights and amounts of aroma β-primeverosides in young leaves and mature leaves of *C. sinensis*.

**Supplemental Table S2.** Summary of the purification of CsGT2 from young fresh leaves of *C. sinensis*.

**Supplemental Table S3.** Gene-specific primers used for 5′ and 3′ RACE, amplification of full-length genes from *C. sinensis*, construction of CsGT2-I141S, or real-time PCR.

**Supplemental Table S4.** Composition of the buffers and solutions for the purification and identification of CsGT2.

**Supplemental Table S5.** GenBank accession numbers used for the construction of the phylogenetic tree in Figure 7.

**Supplemental Materials and Methods S1.** Detailed description of the experimental procedure in this study.

## ACKNOWLEDGMENTS

We thank Drs. Kanzo Sakata (Kyoto University), Tsuyoshi Katsuno (Tea Research Center, Shizuoka Prefectural Research Institute of Agriculture and Forestry), Masahiro Nakao, Nobuo Tsuruoka, Yoshihide Matsuo, Misa Inohara-Ochiai, Masako Fukuchi-Mizutani, Kensuke Tanaka, Naofumi Yoshida, Hitoshi Onuki, and Yuko Fujimori (Suntory, Ltd.), Atsushi Nesumi (Tea Research Center, Makurazaki, Kagoshima Prefecture), Seiji Takahashi and Toru Nakayama (Tohoku University), Hirotomo Kihara and Takao Koeduza (Yamaguchi University), and Koichi Sugimoto and Junji Takabayashi (Kyoto University) for technical support and useful discussions; Drs. Taichi Usui and Takeomi Murata (Shizuoka University) for kindly providing *p*NP-pri, eugenyl-pri, and 2PE-pri; and Dr. Bjoern Hamberger (Copenhagen University) for critical proofreading of the article as well as the Molecular Structure Analysis Section and Functional Genomics Section (Research Institute of Green Science and Technology, Shizuoka University) for LC-MS (LTQ Orbitrap Discovery; Thermo Fisher Scientific), LC-MS/MS (NanoFrontier eLD; Hitachi High-Technology), and gas chromatography-mass spectrometry (JMS-T100GCV; JEOL).

Received March 15, 2015; accepted April 22, 2015; published April 28, 2015.

## LITERATURE CITED

**Aharoni A, Giri AP, Deuerlein S, Griepink F, de Kogel WJ, Verstappen FW, Verhoeven HA, Jongsma MA, Schwab W, Bouwmeester HJ** (2003) Terpenoid metabolism in wild-type and transgenic *Arabidopsis* plants. Plant Cell **15:** 2866–2884

**Arimura G, Matsui K, Takabayashi J** (2009) Chemical and molecular ecology of herbivore-induced plant volatiles: proximate factors and their ultimate functions. Plant Cell Physiol **50:** 911–923

**Balentine DA, Wiseman SA, Bouwens LC** (1997) The chemistry of tea flavonoids. Crit Rev Food Sci Nutr **37:** 693–704

**Bönisch F, Frotscher J, Stanitzek S, Rühl E, Wüst M, Bitz O, Schwab W** (2014a) Activity-based profiling of a physiologic aglycone library reveals sugar acceptor promiscuity of family 1 UDP-glucosyltransferases from grape. Plant Physiol **166:** 23–39

**Bönisch F, Frotscher J, Stanitzek S, Rühl E, Wüst M, Bitz O, Schwab W** (2014b) A UDP-glucose:monoterpenol glucosyltransferase adds to the chemical diversity of the grapevine metabolome. Plant Physiol **165:** 561–581

**Bradford MM** (1976) A rapid and sensitive method for the quantitation of microgram quantities of protein utilizing the principle of protein-dye binding. Anal Biochem **72:** 248–254

**Frey M, Schullehner K, Dick R, Fiesselmann A, Gierl A** (2009) Benzoxazinoid biosynthesis, a model for evolution of secondary metabolic pathways in plants. Phytochemistry **70:** 1645–1651

**Fukushima EO, Seki H, Ohyama K, Ono E, Umemoto N, Mizutani M, Saito K, Muranaka T** (2011) CYP716A subfamily members are multifunctional oxidases in triterpenoid biosynthesis. Plant Cell Physiol **52:** 2050–2061

**Ginglinger JF, Boachon B, Höfer R, Paetz C, Köllner TG, Miesch L, Lugan R, Baltenweck R, Mutterer J, Ullmann P, et al** (2013) Gene coexpression analysis reveals complex metabolism of the monoterpene alcohol linalool in *Arabidopsis* flowers. Plant Cell **25:** 4640–4657

**Graham HN** (1992) Green tea composition, consumption, and polyphenol chemistry. Prev Med **21:** 334–350

**Günata YZ, Bayonove CL, Baumes RL, Cordonnier RE** (1985) The aroma of grapes. I. Extraction and determination of free and glycosidically bound fractions of some grape aroma components. J Chromatogr A **331:** 83–90

**Guo W, Hosoi R, Sakata K, Watanabe N, Yagi A, Ina K, Luo S** (1994) (*S*)-Linalyl, 2-phenylethyl, and benzyl disaccharide glycosides isolated as aroma precursors from oolong tea leaves. Biosci Biotechnol Biochem **58:** 1532–1534

**Guo W, Sakata K, Watanabe N, Nakajima R, Yagi A, Ina K, Luo S** (1993) Geranyl 6-*O*-β-D-xylopyranosyl-β-D-glucopyranoside isolated as an aroma precursor from tea leaves for oolong tea. Phytochemistry **33:** 1373–1375

**Izumi S, Takashima O, Hirata T** (1999) Geraniol is a potent inducer of apoptosis-like cell death in the cultured shoot primordia of *Matricaria chamomilla*. Biochem Biophys Res Commun **259:** 519–522

**Kannangara R, Motawia MS, Hansen NK, Paquette SM, Olsen CE, Møller BL, Jørgensen K** (2011) Characterization and expression profile of two UDP-glucosyltransferases, UGT85K4 and UGT85K5, catalyzing the last step in cyanogenic glucoside biosynthesis in cassava. Plant J **68:** 287–301

**Kawakami M, Ganguly SN, Banerjee J, Kobayashi A** (1995) Aroma composition of oolong tea and black tea by brewed extraction method and characterizing compounds of darjeeling tea aroma. J Agric Food Chem **43:** 200–207

**Kobayashi A, Kubota K, Joki Y, Wada E, Wakabayashi M** (1994) (*Z*)-3-Hexenyl β-D-glucopyranoside in fresh tea leaves as a precursor of green odor. Biosci Biotechnol Biochem **58:** 592–593

**Koeduka T, Suzuki S, Iijima Y, Ohnishi T, Suzuki H, Watanabe B, Shibata D, Umezawa T, Pichersky E, Hiratake J** (2013) Enhancement of production of eugenol and its glycosides in transgenic aspen plants via genetic engineering. Biochem Biophys Res Commun **436:** 73–78

**Koroleva OA, Gibson TM, Cramer R, Stain C** (2010) Glucosinolate-accumulating S-cells in Arabidopsis leaves and flower stalks undergo programmed cell death at early stages of differentiation. Plant J **64:** 456–469

**Krammer G, Winterhalter P, Schwab M, Schreier P** (1991) Glycosidically bound aroma compounds in the fruits of *Prunus* species: apricot (*P. armeniaca*, L.), peach (*P. persica*, L.), yellow plum (*P. domestica*, L. ssp. *Syriaca*). J Agric Food Chem **39:** 778–781

**Kumazawa K, Masuda H** (2002) Identification of potent odorants in different green tea varieties using flavor dilution technique. J Agric Food Chem **50:** 5660–5663

**Lücker J, Bouwmeester HJ, Schwab W, Blaas J, van der Plas LH, Verhoeven HA** (2001) Expression of Clarkia *S*-linalool synthase in transgenic petunia plants results in the accumulation of *S*-linalyl-β-D-glucopyranoside. Plant J **27:** 315–324

**Ma SJ, Mizutani M, Hiratake J, Hayashi K, Yagi K, Watanabe N, Sakata K** (2001) Substrate specificity of β-primeverosidase, a key enzyme in aroma formation during oolong tea and black tea manufacturing. Biosci Biotechnol Biochem **65:** 2719–2729

**Mackenzie PI, Owens IS, Burchell B, Bock KW, Bairoch A, Bélanger A, Fournel-Gigleux S, Green M, Hum DW, Iyanagi T, et al** (1997) The UDP glycosyltransferase gene superfamily: recommended nomenclature update based on evolutionary divergence. Pharmacogenetics **7:** 255–269

**Marlatt C, Ho C, Chien MJ** (1992) Studies of aroma constituents bound as glycosides in tomato. J Agric Food Chem **40:** 249–252

**Mizutani M, Nakanishi H, Ema J, Ma SJ, Noguchi E, Inohara-Ochiai M, Fukuchi-Mizutani M, Nakao M, Sakata K** (2002) Cloning of β-primeverosidase from tea leaves, a key enzyme in tea aroma formation. Plant Physiol **130:** 2164–2176

**Mizutani M, Ward E, Ohta D, inventors.** March 27, 1997. Plant geraniol/nerol 10-hydroxylase and DNA coding therefor. European Patent Application No. 96931058.0

**Montefiori M, Espley RV, Stevenson D, Cooney J, Datson PM, Saiz A, Atkinson RG, Hellens RP, Allan AC** (2011) Identification and characterisation of F3GT1 and F3GGT1, two glycosyltransferases responsible for anthocyanin biosynthesis in red-fleshed kiwifruit (*Actinidia chinensis*). Plant J **65:** 106–118

**Moon JH, Watanabe N, Ijima Y, Yagi A, Sakata K** (1996) *Cis*- and *trans*-linalool 3,7-oxides and methyl salicylate glycosides and (*Z*)-3-hexenyl β-D-glucopyranoside as aroma precursors from tea leaves for oolong tea. Biosci Biotechnol Biochem **60:** 1815–1819

**Moon JH, Watanabe N, Sakata K, Yagi A, Ina K, Luo S** (1994) *Trans*- and *cis*-linalool 3,6-oxide 6-*O*-β-D-xylopyranosyl-β-D-glucopyranosides isolated as aroma precursors from leaves for oolong tea. Biosci Biotechnol Biochem **58:** 1742–1744

**Morita Y, Hoshino A, Kikuchi Y, Okuhara H, Ono E, Tanaka Y, Fukui Y, Saito N, Nitasaka E, Noguchi H, et al** (2005) Japanese morning glory dusky mutants displaying reddish-brown or purplish-gray flowers are deficient in a novel glycosylation enzyme for anthocyanin biosynthesis, UDP-glucose:anthocyanidin 3-*O*-glucoside-2′′-*O*-glucosyltransferase, due to 4-bp insertions in the gene. Plant J **42:** 353–363

**Murata T, Shimada M, Watanabe N, Sakata K, Usui T** (1999) Practical enzymatic synthesis of primeverose and its glycoside. J Appl Glycosci **46:** 431–437

**Noguchi A, Fukui Y, Iuchi-Okada A, Kakutani S, Satake H, Iwashita T, Nakao M, Umezawa T, Ono E** (2008) Sequential glucosylation of a furofuran lignan, (+)-sesaminol, by *Sesamum indicum* UGT71A9 and UGT94D1 glucosyltransferases. Plant J **54:** 415–427

**Noguchi A, Horikawa M, Fukui Y, Fukuchi-Mizutani M, Iuchi-Okada A, Ishiguro M, Kiso Y, Nakayama T, Ono E** (2009) Local differentiation of sugar donor specificity of flavonoid glycosyltransferase in Lamiales. Plant Cell **21:** 1556–1572

**Obayashi T, Nishida K, Kasahara K, Kinoshita K** (2011) ATTED-II updates: condition-specific gene coexpression to extend coexpression analyses and applications to a broad range of flowering plants. Plant Cell Physiol **52:** 213–219

**Offen W, Martinez-Fleites C, Yang M, Kiat-Lim E, Davis BG, Tarling CA, Ford CM, Bowles DJ, Davies GJ** (2006) Structure of a flavonoid glucosyltransferase reveals the basis for plant natural product modification. EMBO J **25:** 1396–1405

**Ohgami S, Ono E, Toyonaga H, Watanabe N, Ohnishi T** (2014) Identification and characterization of *Camellia sinensis* glucosyltransferase, UGT73A17: a possible role in flavonol glucosylation. Plant Biotechnol **31:** 573–578

**Ono E, Homma Y, Horikawa M, Kunikane-Doi S, Imai H, Takahashi S, Kawai Y, Ishiguro M, Fukui Y, Nakayama T** (2010a) Functional differentiation of the glycosyltransferases that contribute to the chemical diversity of bioactive flavonol glycosides in grapevines (*Vitis vinifera*). Plant Cell **22:** 2856–2871

**Ono E, Ruike M, Iwashita T, Nomoto K, Fukui Y** (2010b) Co-pigmentation and flavonoid glycosyltransferases in blue *Veronica persica* flowers. Phytochemistry **71:** 726–735

**Osmani SA, Bak S, Imberty A, Olsen CE, Møller BL** (2008) Catalytic key amino acids and UDP-sugar donor specificity of a plant glucuronosyltransferase, UGT94B1: molecular modeling substantiated by site-specific mutagenesis and biochemical analyses. Plant Physiol **148:** 1295–1308

**Pabst A, Barron A, Etievant P, Schreier P** (1991) Studies on the enzymatic hydrolysis of bound aroma constituents from raspberry fruit pulp. J Agric Food Chem **39:** 173–175

**Pattnaik S, Subramanyam VR, Bapaji M, Kole CR** (1997) Antibacterial and antifungal activity of aromatic constituents of essential oils. Microbios **89:** 39–46

**Pichersky E, Gershenzon J** (2002) The formation and function of plant volatiles: perfumes for pollinator attraction and defense. Curr Opin Plant Biol **5:** 237–243

**Roscher R, Herderich M, Steffen JP, Schreier P, Schwab W** (1996) 2,5-Dimethyl-4-hydroxy-3[2H]-furanone 6′*O*-malonyl-β-D-glucopyranoside in strawberry fruits. Phytochemistry **43:** 155–159

**Sawada S, Suzuki H, Ichimaida F, Yamaguchi MA, Iwashita T, Fukui Y, Hemmi H, Nishino T, Nakayama T** (2005) UDP-glucuronic acid:anthocyanin glucuronosyltransferase from red daisy (*Bellis perennis*) flowers: enzymology and phylogenetics of a novel glucuronosyltransferase involved in flower pigment biosynthesis. J Biol Chem **280:** 899–906

**Sayama T, Ono E, Takagi K, Takada Y, Horikawa M, Nakamoto Y, Hirose A, Sasama H, Ohashi M, Hasegawa H, et al** (2012) The *Sg-1* glycosyltransferase

locus regulates structural diversity of triterpenoid saponins of soybean. Plant Cell **24:** 2123–2138

**Shibuya M, Nishimura K, Yasuyama N, Ebizuka Y** (2010) Identification and characterization of glycosyltransferases involved in the biosynthesis of soyasaponin I in *Glycine max*. FEBS Lett **584:** 2258–2264

**Sugimoto K, Matsui K, Iijima Y, Akakabe Y, Muramoto S, Ozawa R, Uefune M, Sasaki R, Alamgir KM, Akitake S, et al** (2014) Intake and transformation to a glycoside of (*Z*)-3-hexenol from infested neighbors reveals a mode of plant odor reception and defense. Proc Natl Acad Sci USA **111:** 7144–7149

**Tamura K, Stecher G, Peterson D, Filipski A, Kumar S** (2013) MEGA6: Molecular Evolutionary Genetics Analysis version 6.0. Mol Biol Evol **30:** 2725–2729

**Tikunov YM, Molthoff J, de Vos RC, Beekwilder J, van Houwelingen A, van der Hooft JJ, Nijenhuis-de Vries M, Labrie CW, Verkerke W, van de Geest H, et al** (2013) NON-SMOKY GLYCOSYLTRANSFERASE1 prevents the release of smoky aroma from tomato fruit. Plant Cell **25:** 3067–3078

**Tsukada T, Igarashi K, Yoshida M, Samejima M** (2006) Molecular cloning and characterization of two intracellular β-glucosidases belonging to glycoside hydrolase family 1 from the basidiomycete *Phanerochaete chrysosporium*. Appl Microbiol Biotechnol **73:** 807–814

**Usadel B, Obayashi T, Mutwil M, Giorgi FM, Bassel GW, Tanimoto M, Chow A, Steinhauser D, Persson S, Provart NJ** (2009) Co-expression tools for plant biology: opportunities for hypothesis generation and caveats. Plant Cell Environ **32:** 1633–1651

**Wang D, Yoshimura T, Kubota K, Kobayashi A** (2000) Analysis of glycosidically bound aroma precursors in tea leaves. 1. Qualitative and quantitative analyses of glycosides with aglycons as aroma compounds. J Agric Food Chem **48:** 5411–5418

**Yano M, Joki Y, Mutoh H, Kubota K, Kobayashi A** (1991) Benzyl glucoside from tea leaves. Agric Biol Chem **55:** 1205–1206

**Yauk YK, Ged C, Wang MY, Matich AJ, Tessarotto L, Cooney JM, Chervin C, Atkinson RG** (2014) Manipulation of flavour and aroma compound sequestration and release using a glycosyltransferase with specificity for terpene alcohols. Plant J **80:** 317–330

**Yonekura-Sakakibara K, Fukushima A, Nakabayashi R, Hanada K, Matsuda F, Sugawara S, Inoue E, Kuromori T, Ito T, Shinozaki K, et al** (2012) Two glycosyltransferases involved in anthocyanin modification delineated by transcriptome independent component analysis in Arabidopsis thaliana. Plant J **69:** 154–167

**Yonekura-Sakakibara K, Hanada K** (2011) An evolutionary view of functional diversity in family 1 glycosyltransferases. Plant J **66:** 182–193

**Yonekura-Sakakibara K, Nakabayashi R, Sugawara S, Tohge T, Ito T, Koyanagi M, Kitajima M, Takayama H, Saito K** (2014) A flavonoid 3-*O*-glucoside:2′′-*O*-glucosyltransferase responsible for terminal modification of pollen-specific flavonols in Arabidopsis thaliana. Plant J **79:** 769–782

**Yonekura-Sakakibara K, Tanaka Y, Fukuchi-Mizutani M, Fujiwara H, Fukui Y, Ashikari T, Murakami Y, Yamaguchi M, Kusumi T** (2000) Molecular and biochemical characterization of a novel hydroxycinnamoyl-CoA:anthocyanin 3-*O*-glucoside-6′′-*O*-acyltransferase from *Perilla frutescens*. Plant Cell Physiol **41:** 495–502

**Young H, Paterson VJ** (1995) Characterization of bound flavour components in kiwifruit. J Sci Food Agric **68:** 257–260